Advances in Nano Research, *Vol. 12, No. 1 (2022) 65-72*
https://doi.org/10.12989/anr.2022.12.1.065

The determination of effect of TiO_2 on dynamic behavior of scaled WPC warehouse by OMA

Sertaç Tuhta*

Ondokuz Mayis University, Faculty of Engineering, Department of Civil Engineering, Atakum/Samsun, Turkey

(*Received October 1, 2021, Revised November 2, 2021, Accepted November 3, 2021*)

Abstract. The dynamic properties (frequencies, mode shapes, damping ratios) of the scaled WPC warehouse are compared using the operational modal analysis approach to the dynamic parameters (frequencies, mode shapes, damping ratios) of the full outer surface of titanium dioxide, 70 micron in thickness. Micro tremor ambient vibration data on ground level was used to provide ambient excitation. For the output-only modal identification, Enhanced Frequency Domain Decomposition (EFDD) was used. This study discovered a strong correlation between mode shapes. Titanium dioxide applied to the entire outer surface of the scaled WPC warehouse results in an average 14.05 percent difference in frequency values and 7.61 percent difference in damping ratios, demonstrating that nanomaterials can be used to increase rigidity in structures, or for reinforcement. Another significant finding in the study was the highest level of adherence of titanium dioxide and similar nanomaterials mentioned in the introduction to WPC structure surfaces.

Keywords: EFDD; nanomaterial; operational modal analysis; TiO_2; WPC

1. Introduction

Because nanotechnology is a rapidly evolving field, it is difficult to provide a broad definition. However, according to the definition that everyone agrees on, nanotechnology is the production of materials and devices by controlling the substance. At the atomic, molecular, and supramolecular (nanoscale) levels, it can be expressed as the use of very small material particles to create new large-scale materials. Nanomaterials are products created using nanotechnologies. Nanotechnology is defined as the study and application of structures ranging in size from 1 nanometer (nm) to 100 nanometers. Various issues arise during nano-level processing, such as gravity becoming insignificant, the emergence of electrostatic forces, and the emergence of quantum effects (Xiong *et al*. 2013, Lin *et al*. 2015). Another significant point is that, as a result of the use of nanoscale particles, the ratio of atoms on the surface to those inside increases, causing the material properties to change. Nanotechnology can create materials with many unique properties that can improve existing building materials, such as lighter and stronger structural composites, low-maintenance coatings, more useful cement-based materials, and products with better thermal insulation properties, to name a few (Wang *et al*. 2018, Hussain *et al*. 2019). The incorporation of nanomaterials into the composition of some materials, such as cement, concrete, and WPC, will benefit air conditioning and energy efficiency. Furthermore, nanomaterials applied to the surfaces of building structural elements can contribute to environmental cleaning and energy generation via photocatalytic reactions (Guo *et al*. 2019, Akbaş 2020). Concrete can be made stronger, more durable, and easier to install thanks to nanotechnology, steel can be made tougher, self-cleaning glass can be made, and paints can be made more insulating and water-repellent. Because of the new potential applications of nanometer-scale particles, nano-materials and nanotechnologies have sparked a lot of scientific interest, as well as a lot of funding and effort. The construction industry has lagged behind other large industrial sectors in terms of its potential to benefit from nanotechnology. The following are reports on the use of nanotechnology in construction materials, as well as potential uses of nanotechnology in the construction and development of building materials: Using nanoparticles, carbon nanotubes, and nanofibers to improve the strength and durability of cement composites while reducing environmental pollution; producing cheap and corrosion-free steel; producing products with ten times the performance of existing thermal insulation materials; and producing coatings that enable self-cleaning and self-color change to reduce energy consumption. The use of nanotechnological materials in buildings not only increases their life span, but also allows them to respond to various factors such as energy savings, fire resistance, and corrosion. When compared to silica fume (microsilica), nano-silica shortens the setting time of mortar and reduces mixing water and segregation by improving cohesion (Zhang *et al*. 2020, 2021, Wang *et al*. 2021). Current nanoscience and nanotechnology researchers are delving deeply into these novel properties (Eltaher *et al*. 2019). Because macro properties can change at the nanoscale, significantly new materials and processes can be created. Discussions about the application of nanotechnology in civil engineering, particularly in construction, are critical. Many advances in nanotechnology, however, have the

*Corresponding author, Assistant Professor,
E-mail: stuhta@omu.edu.tr

ISSN: 2287-237X (Print), 2287-2388 (Online)

potential to be applied in the field of civil engineering. The use of nanotechnological materials in buildings not only increases their life span, but also allows them to respond to various factors such as energy consumption, fire resistance, and corrosion. Using nanotechnological materials, you can avoid a variety of negative effects that occur with time in building elements (self-healing and waterproof concrete, self-cleaning plaster, etc.) Aydogdu and Eren (2018). According to the information provided above, carbon nanotubes, one of the most commonly used nanomaterials in the field of civil engineering, are cylindrical carbon tubes that get their name from their nanometer diameter. They can be several millimeters long and have a "layer" or wall (single wall nanotubes) or multiple walls (multi-wall nanotubes), according to (Uzun and Civalek 2019, Civalek *et al*. 2020, Hussain *et al*. 2020a, b, c). Nanotubes have exceptional strength, unique electrical properties, and efficient thermal properties. Because of its properties, it is extremely popular. Another nanomaterial, titanium dioxide nanoparticles, is used to improve the properties of concrete. Because of its sterilizing properties, this white pigment is used as a very good reflective coating or added to paints, cement, and windows. Titanium dioxide, when applied to external surfaces, degrades organic pollutants, volatile organic compounds, and bacterial membranes via powerful photocatalytic reactions and reduces the proportion of air pollutants. Because it is hydrophilic, it provides a self-cleaning feature to the surfaces on which it is used. The obtained concrete surfaces have a white color that effectively preserves their whiteness. Silicon dioxide particles, on the other hand, have the ability to significantly increase compressive strength. They enable the production of concrete containing large amounts of fly ash at an early stage by filling the pores between large fly ash and cement particles. When compared to silica fume (microsilica), nano-silica shortens the setting time of mortar and reduces mixing water and segregation by improving cohesion (Ma *et al*. 2016, Wang *et al*. 2020). Because of their semiconductor and piezoelectric properties, zinc oxides are preferred. They are used in a variety of building materials, including plastics, ceramics, glass, cement, rubber, paints, adhesives, sealants, pigments, and flame retardants. Zinc oxide used in concrete production shortens the processing time and increases water resistance. Alumina, another nanomaterial, reacts with calcium hydroxide, which is formed during the hydration of calcium silicates. The rate of the pozzolanic reaction is proportional to the available surface area for the reaction. The addition of high purity nano-alumina improves the properties of concretes by increasing tensile and flexural strength. Cement can be advantageously replaced in the concrete mix with nano-alumina particles up to a maximum of 2.0 percent with average particle sizes of 15 nm; 1.0 percent replacement yields the highest nano-alumina particle content. When academic studies on the subject have been examined, it has been determined that there is no significant accumulation of nanomaterials in the field of applied civil engineering (Pandey *et al*. 2019). As a result, a study with no precedents in the literature was conducted on this study. The operational modal analysis method was used to determine the dynamic parameters (frequencies, mode shapes, and damping ratios) of a scaled WPC warehouseIn a subsequent study, the upper surface of this structure was coated with titanium dioxide (70 micron), and its dynamic parameters (frequencies, mode shapes, damping ratios) were determined and compared using the operational modal analysis method. The reason for using titanium dioxide in the study is that its mechanical properties are comparable to those of conventional reinforcement materials (AFRP, BFRP, CFRP, GFRP, etc.). Details that will aid those working on this subject have been included as a result of the research. Other nanomaterials, such as titanium dioxide, are being investigated for use as reinforcement elements in concrete, reinforced concrete, steel, composite-type structures, and WPC, and the results of these studies will be presented later. Ambient vibration testing (also known as Operational Modal Analysis) is the most cost-effective, non-destructive method for collecting vibration data from large civil engineering structures for Output-Only Modal Identification. In Vibration of Buildings, general characteristics of structural response (appropriate frequency, displacement, velocity, acceleration), suggested measuring quantity (such as velocity or acceleration) depends on the type of vibrations (Traffic, Acoustic, Machinery inside, Earthquakes, Wind...) are given (1990).

In general, operational modal analysis is used to determine the damage levels of the existing structures, to check the validity of the assumptions made while constructing the finite element model, to update the initial numerical model of the existing structures according to the experimental data, to determine the dynamic characteristics of the structures by the experimental modal analysis method when the numerical model of the existing structures cannot be formed and to follow the structural health is widely used in the process Alvin and Park (1994), Tseng *et al*. (1994), Aliev and Larin (1998), Ljung (1999), Lus *et al*. (2003), Roeck (2003). The engineering structures used three types of definitions: modal parameter identification, structural-modal parameter identification, and control-model identification methods. The system identification in the frequency domain is based on the singular value decomposition of the spectral density matrix and is known as Frequency Domain Decomposition (FDD), and its further development is known as Enhanced Frequency Domain Decomposition (EFDD). The Stochastic Subspace Identification (SSI) technique has three different time domain implementations: Sestieri and Ibrahim (1994), Balmes (1997), Bendat (1998), Marwala (1998) use Unweighted Principal Component (UPC); Principal Component (PC); Canonical Variety Analysis (CVA) for modal updating of the structure (2010).

It is necessary to estimate the sensitivity of the examined system's reaction to changing the random or fuzzy parameters of a structure. The effects of measurement noise perturbation on the identified system modal and physical parameters were investigated. Estimated measurement noise border, for which identified system parameters are acceptable for validation of the examine system's finite element model. The observer Kalman filter Kalman (1960), Trifunac (1972), Ibrahim (1977) and Juang

(1994) Subspace algorithms are used to identify the system. In some cases, the observer gain and the Kalman gain may coincide. The Monte-Carlo method is used to simulate the structure's stochastic state-space model. As a result of these theoretical and experimental studies, the importance of temperature change and humidity as environmental factors affecting the modal parameters has emerged once more. Temperature and humidity effects on modal parameters have been thoroughly investigated over the last 15 years Kasmzade and Tuhta (2017), Tuhta (2018, 2019). The operational modal analysis method is used to compare the dynamic parameters (frequencies, mode shapes, damping ratios) of the scaled WPC warehouse and the dynamic parameters (frequencies, mode shapes, damping ratios) of the entire outer surface of the 70 micron thick titanium dioxide. The recorded micro tremor ambient vibration data on ground level provided ambient excitation. For output-only modal identification, Enhanced Frequency Domain Decomposition (EFDD) is used.

2. Modal parameter extractions (EFDD)

The (FDD) ambient modal identification technique is a variation on the Basic Frequency Domain (BFD) technique, also known as the Peak-Picking technique. In the case of a white noise input and a lightly damped structure, this method makes use of the fact that modes can be estimated from the calculated spectral densities. It is a non-parametric technique for determining modal parameters directly from signal processing. Using a Singular Value Decomposition (SVD) of each measurement data set, the FDD technique estimates the modes. For each singular value, this decomposition corresponds to a Single Degree of Freedom (SDOF) identification of the measured system (Brincker *et al*. 2000). The Enhanced Frequency Domain Decomposition technique is an extension to Frequency Domain Decomposition (FDD) technique. This technique is a simple technique that is extremely basic to use. In this technique, modes are easily picked locating the peaks in Singular Value Decomposition (SVD) plots calculated from the spectral density spectra of the responses. FDD technique is based on using a single frequency line from the Fast Fourier Transform analysis (FFT), the accuracy of the estimated natural frequency based on the FFT resolution and no modal damping is calculated. On the other hand, EFDD technique gives an advanced estimation of both the natural frequencies, the mode shapes and includes the damping ratios (Jacobsen *et al*. 2006). In EFDD technique, the single degree of freedom (SDOF) Power Spectral Density (PSD) function, identified about a peak of resonance, is taken back to the time domain using the Inverse Discrete Fourier Transform (IDFT). The natural frequency is acquired by defining the number of zero crossing as a function of time, and the damping by the logarithmic decrement of the correspondent single degree of freedom (SDOF) normalized auto correlation function Peeters (2000). In this study modal parameter identification was implemented by the Enhanced Frequency Domain Decomposition. The relationship between the input and responses in the EFDD technique can be written as, in this method, unknown input is represented with $x(t)$ and measured output is represented with $y(t)$

$$\left[G_{yy}(j\omega)\right]=[H(j\omega)]^{*}[G_{xx}(j\omega)][H(j\omega)]^{T} \tag{1}$$

where $G_{xx}(j\omega)$ is the $r\,x\,r$ Power Spectral Density (PSD) matrix of the input. $G_{yy}(j\omega)$ is the $m\,x\,m$ Power Spectral Density (PSD) matrix of the output, $H(j\omega)$ is the $m\,x\,r$ Frequency Response Function (FRF) matrix, and * and superscript T denote complex conjugate and transpose, respectively. The FRF can be reduced to a pole/residue form as follows:

$$[H(\omega)]=\frac{[Y(\omega)]}{[X(\omega)]}=\sum_{k=1}^{m}\frac{[R_k]}{j\omega-\lambda_k}+\frac{[R_k]^{*}}{j\omega-\lambda_k^{*}} \tag{2}$$

where n is the number of modes λ_k is the pole and, R_k is the residue. Then Eq. (1) becomes as:

$$G_{yy}(j\omega)=\sum_{k=1}^{n}\sum_{s=1}^{n}\left[\frac{[R_k]}{j\omega-\lambda_k}+\frac{[R_k]^{*}}{j\omega-\lambda_k^{*}}\right] G_{xx}(j\omega)\left[\frac{[R_s]}{j\omega-\lambda_s}+\frac{[R_s]^{*}}{j\omega-\lambda_s^{*}}\right]^{\bar{H}} \tag{3}$$

where s the singular values, superscript is H denotes complex conjugate and transpose. Multiplying the two partial fraction factors and making use of the Heaviside partial fraction theorem, after some mathematical manipulations, the output PSD can be reduced to a pole/residue form as fallows;

$$E\left[G_{yy}(j\omega)\right]=\sum_{k=1}^{n}\frac{[A_k]}{j\omega-\lambda_k}+\frac{[A_k]^{*}}{j\omega-\lambda_k^{*}}+\frac{[B_k]}{-j\omega-\lambda_k}+\frac{[B_k]^{*}}{-j\omega-\lambda_k^{*}} \tag{4}$$

where A_k is the k th residue matrix of the output PSD. In the EFDD identification, the first step is to estimate the PSD matrix. The estimation of the output PSD known at discrete frequencies is then decomposed by taking the SVD (singular value decomposition) of the matrix;

$$G_{yy}(j\omega_i) = U_i S_i U_i^{\bar{H}} \tag{5}$$

where the matrix $U_i = [u_{i1},u_{i2}, \ldots ,u_{im}]$ is a unitary matrix holding the singular vectors u_{ij} and s_{ij} is a diagonal matrix holding the scalar singular values. The first singular vector u_{ij} is an estimation of the mode shape. PSD function is identified around the peak by comparing the mode shape estimation u_{ij} with the singular vectors for the frequency lines around the peak. From the piece of the SDOF density function obtained around the peak of the PSD, the natural frequency and the damping can be obtained.

3. Description of the scaled WPC warehouse

The scaled WPC warehouse was obtained in the Ondokuz Mayıs University Civil Engineering Laboratory. The mechanical properties of the WPC used are as follows: modulus of elasticity E = 2.0E9 N/m^2, Poisson ratio μ = 0.35, mass per unit volume ρ = 10000 N/m^3. The dimensions of the building are shown in Fig. 1.

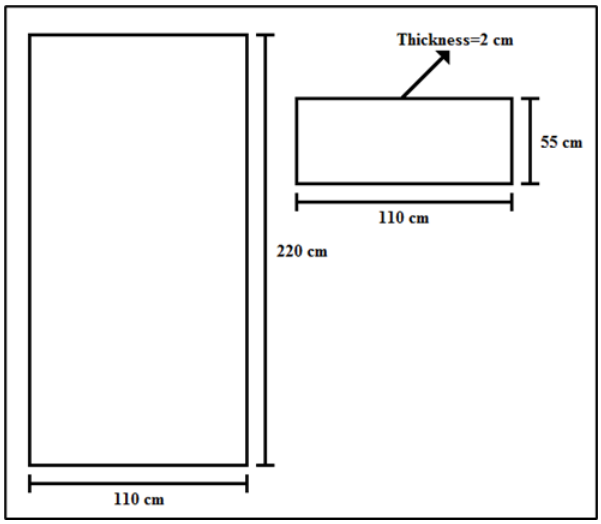

Fig. 1 Illustration of the scaled WPC warehouse

(a) First setup

(b) Second setup

Fig. 2 The accelerometers location of the experimental model in the 3D view

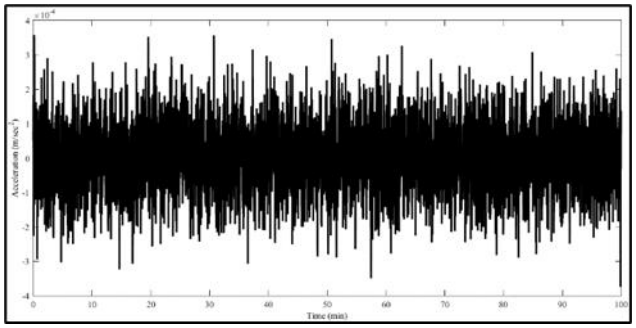

Fig. 3 Ambient excitation data from the recorded micro tremor data on ground level x axis-time (min), y axis-acceleration (m/sec^2)

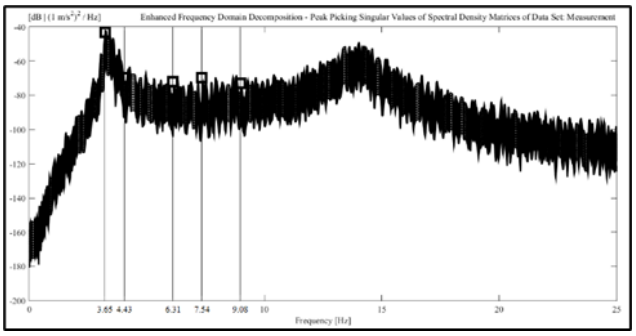

Fig. 4 Singular values of spectral density matrices (scaled WPC warehouse) x axis-frequency (hz), y axis-[db|(1 m/s^2)^2/hz]

4. Operational modal analysis of the scaled WPC warehouse

Three accelerometers were used to measure ambient vibrations. One of them is always assigned as the reference sensor located at the bottom of shear wall. The acceleration record was measured in two data setsTwo and three accelerometers were used for the two data sets, respectively. Accelerometers were calibrated and used, thus preventing possible measurement errors. 6000 seconds were recorded for each data set. Selected measurement points and directions are shown in the figure. Ambient simulation was achieved using micro tremor data recorded at ground level.

After the first data set measurement, the accelerometers were recalibrated. The acceleration records of the first data set were saved in the folder for analysis. Before starting the second data set measurement, all connections were rechecked.

The data acquisition computer generates the ambient vibration records. During measurements, the data files from the previous setup are transferred to the computer for data analysis using a software package. However, if the data set exhibits unexpected signal drifts, unwanted noise, or is corrupted for unknown reasons, it must be discarded and measurements must be repeated. Before measurements were made, the cable used to connect the sensors to the data acquisition equipment must be laid out. Following each measurement, the roving sensors are systematically located from floor to floor until the test is completed (Figs. 2(a) and (b)). The equipment used for the measurement includes three Sensebox accelerometers (with both *x* and *y* directional measurements) and Güralp systems seismometer and Matlab Data acquisition toolbox. For modal parameter estimation from the ambient vibration data, the operational modal analysis (OMA) software ARTeMIS Extractor (1999) is used. The Eigen frequencies were found as the peaks of non-parametric spectrum estimates when the simple peak-picking method (PPM) was used.

In the presence of noisy test data, weakly excited modes, and relatively close Eigen frequencies, this frequency selection procedure became subjective. The related half-power bandwidth method was also unsuitable for estimating damping ratios. Because of its convenience and operating speed, Frequency Domain Decomposition (FDD) is the most popular and useful algorithm to use.

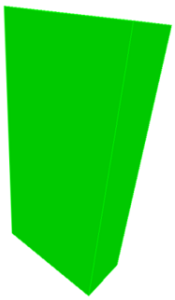

1st Mode shape (f = 3.65 Hz, ξ = 0.92)

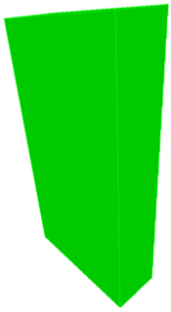

2nd Mode shape (f = 4.43 Hz, ξ = 0.76)

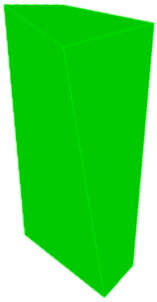

3rd Mode shape (f = 6.31 Hz, ξ = 0.59)

4th Mode shape (f = 7.54 Hz, ξ = 0.68)

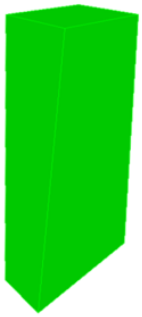

5th Mode shape (f = 9.08 Hz, ξ = 0.52)

Fig. 5 Experimentally identified mode shapes of the scaled WPC warehouse

Table 1 Operational modal analysis result at the scaled WPC warehouse

Mode number	1	2	3	4	5
Frequency (Hz)	3.65	4.43	6.31	7.54	9.08
Modal damping ratio (ξ)	0.92	0.76	0.59	0.68	0.52

Fig. 6 Materials and equipment used in coating application

Singular values of spectral density matrices, attained from vibration data using PP (Peak Picking) technique were shown in Fig. 4. Natural frequencies acquired from all measurement setup were given in Table 1. The first five mode shapes extracted from experimental modal analyses were given in Fig. 5. When all measurements were examined, it could be seen that a good accordance was found between experimental mode shapes. In addition, when both setup sets were experimentally identified modal parameters were checked with each other, it could be seen that there was a best agreement between the mode shapes in the experimental modal analyses.

5. Operational modal analysis of the coated scaled WPC warehouse

In the case of the coated scaled WPC warehouse, the following studies were made on it to check and examine the efficiency of using TiO_2 coating: the entire outer surface of the 70 micron thick of the structure were coated with multi-layer TiO_2 coating. TiO_2 coating and its components YKS is a product of YKS (Yapı Kimyasalları Sanayi) corporation, Bosch branded PFS2000 model spray equipment was used in the coating application (Fig. 6). The properties of the TiO_2 coating are: E = 23E10 N/m^2, Poisson ratio μ = 0.27, mass per unit volume ρ = 40000 N/m^3, thickness = 0.00008 m.

Many layers of titanium dioxide cover the entire outer surface of the scaled WPC warehouse. During each application, the surface is expected to dry. 1 hour of curing time is required to prepare a surface for the application of titanium dioxide. Following these setups, ambient vibration tests are performed, followed by curing to obtain experimental dynamic properties that are similar to previously used properties in order to obtain comparative measurements. SVSDM are shown in Fig. 7. Table 2 shows the identified natural frequencies and modal damping ratios.

It is clear that using titanium dioxide seems to be very effective for strengthening WPC members along with increasing stiffness; this research aims to determine how

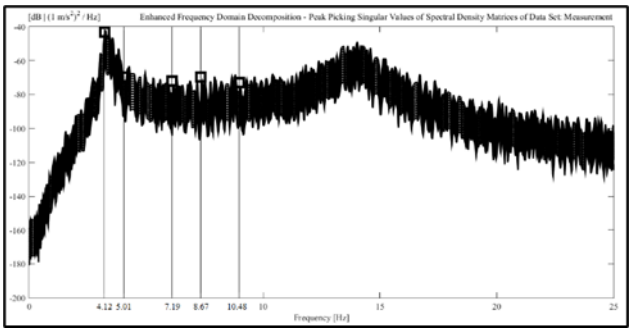

Fig. 7 Singular values of spectral density matrices (coated scaled WPC warehouse) x axis-frequency (hz), y axis-[db|(1 m/s^2)^2/hz]

Table 2 Operational modal analysis result at the coated scaled WPC warehouse

Mode number	1	2	3	4	5
Frequency (Hz)	3.65	4.43	6.31	7.54	9.08
Modal damping ratio (ξ)	0.92	0.76	0.59	0.68	0.52

Table 3 Comparison of the existing and the coated structures frequency results

Mode number	1	2	3	4	5
Frequency (Hz)-E	3.65	4.43	6.31	7.54	9.08
Frequency (Hz)-C	4.12	5.01	7.19	8.67	10.48
Difference (%)	12.87	13.09	13.94	14.98	15.41

Table 4 Comparison of the existing and the coated structures damping ratio results

Mode number	1	2	3	4	5
Modal damping ratio (ξ)-E	0.92	0.76	0.59	0.68	0.52
Modal damping ratio (ξ)-C	0.82	0.74	0.63	0.70	0.59
Difference (%)	12.19	2.70	6.77	2.94	13.46

TiO_2 implementation affects structural response of the scaled WPC warehouse by changing its dynamic characteristics.

6. Conclusions

In this study, operational modal analysis of the existing and titanium dioxide coated scaled WPC warehouse was performed and the results were evaluated. In the comparison of the result of this study, the followings were observed:

• From the ambient vibration test, the first five natural frequencies are attained experimentally, which range between 3 and 11 Hz.

• When comparing the existing and coated scaled WPC warehouse results, it is clear that the mode shapes are in good agreement (Figs. 7 and 8).

• It has been determined that there is an average of14.05% difference between the frequency values of the existing scaled WPC warehouse and the titanium dioxide coated scaled WPC warehouse.

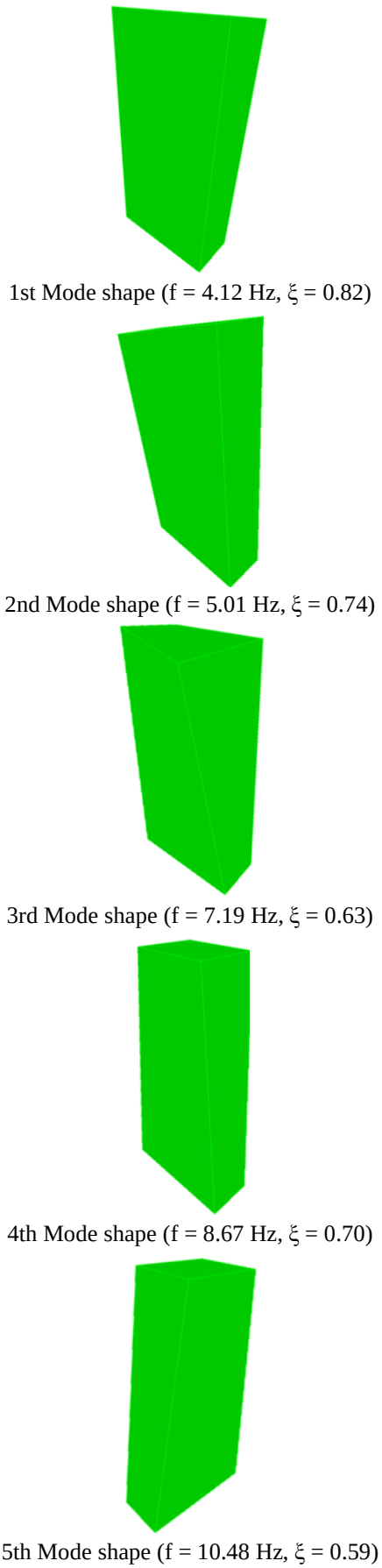

1st Mode shape (f = 4.12 Hz, ξ = 0.82)

2nd Mode shape (f = 5.01 Hz, ξ = 0.74)

3rd Mode shape (f = 7.19 Hz, ξ = 0.63)

4th Mode shape (f = 8.67 Hz, ξ = 0.70)

5th Mode shape (f = 10.48 Hz, ξ = 0.59)

Fig. 8 Experimentally identified mode shapes of the coated scaled WPC warehouse

• It has been determined that there is an average of 7.61% difference between the damping ratios of the existing scaled WPC warehouse and the titanium dioxide coated scaled WPC warehouse.

• Titanium dioxide applied to the entire outer surface (70 micron thick) of the scaled WPC warehouse has an average of 14.05% difference in frequency values (Table 3) and 7.61% in damping ratios (Table 4), proving that nanomaterials can be used to increase rigidity in structures, in other words, for reinforcement.

• Another significant finding in the study was the highest level of adherence of titanium dioxide and similar nanomaterials mentioned in the introduction to WPC structure surfaces.

References

Akbaş, Ş.D. (2020), "Modal analysis of viscoelastic nanorods under an axially harmonic load", *Adv. Nano Res.*, **8**(4), 277-282. https://doi.org/10.12989/anr.2020.8.4.277.

Aliev, F.A. and Larin, V.B. (1998), *Optimization of Linear Control Systems: Analytical Methods and Computational Algorithms*, CRC Press, Florida, U.S.A.

Alvin, K.F. and Park, K.C. (1994), "Second-order structural identification procedure via state-space-based system identification", *AIAA Journal*, **32**(2), 397-406. https://doi.org/10.2514/3.11997.

ANSI S2.47 (1990), Vibration of buildings-guidelines for the measurement of vibrations and evaluation of their effects on buildings, American National Standards Institute; Washington, DC, U.S.A.

ARTeMIS (2004), Ambient Response Testing and Modal Identification Software ARTeMIS Extractor 3.3.; Structural Vibration Solution A/S Aalborg East, Denmark. www.svibs.com

Balmes, E. (1997), "New results on the identification of normal modes from experimental complex modes", *Mech. Syst. Signal Proc.*, **11**(2), 229-243. https://doi.org/10.1006/mssp.1996.0058.

Bendat, J.S. (1998), *Nonlinear Systems Techniques and Applications*, Wiley, New Jersey, U.S.A.

Brincker, R., Zhang, L. and Andersen, P. (2000), "Modal identification from ambient responses using frequency domain decomposition", *Proceedings of the 18th International Modal Analysis Conference* (*IMAC)*, Texas, U.S.A., February.

Civalek, O., Uzun, B. and Yayli, M.O. (2020), "Frequency, bending and buckling loads of nanobeams with different cross sections", *Adv. Nano Res.*, **9**(2), 91-104. https://doi.org/10.12989/anr.2020.9.2.091.

Eltaher, M.A., Almalki, T.A., Ahmed, K.I. and Almitani, K.H. (2019), "Characterization and behaviors of single walled carbon nanotube by equivalent-continuum mechanics approach", *Adv. Nano Res.*, **7**(1), 39-49. https://doi.org/10.12989/anr.2020.7.1.039.

Eren, M. and Aydogdu, M. (2018), "Finite strain nonlinear longitudinal vibration of nanorods", *Adv. Nano Res.*, **6**(4), 323-337. https://doi.org/10.12989/anr.2018.6.4.323.

Guo, Y., He, D., Xie, A., Qu, W., Tang, Y., Zhou, L. and Zhu, R. (2019), "The electrochemical oxidation of hydroquinone and catechol through a novel poly-geminal dicationic ionic liquid (PGDIL)–TiO_2 composite film electrode", *Polymers*, **11**(11), 1907. https://doi.org/10.3390/polym11111907.

Hussain, M., Naeem, M.N., Tounsi, A. and Taj, M. (2019), "Nonlocal effect on the vibration of armchair and zigzag SWCNTs with bending rigidity", *Adv. Nano Res.*, **7**(6), 431-442. https://doi.org/10.12989/anr.2019.7.6.431.

Hussain, M., Naeem, M.N., Taj, M. and Tounsi, A. (2020a), "Simulating vibration of single-walled carbon nanotube using Rayleigh-Ritz's method", *Adv. Nano Res.*, **8**(3), 215-228. https://doi.org/10.12989/anr.2020.8.3.215

Hussain, M., Naeem, M.N. and Tounsi, A. (2020b), "Response of orthotropic Kelvin modeling for single-walled carbon nanotubes: Frequency analysis", *Adv. Nano Res.*, **8**(3), 229-244. https://doi.org/10.12989/anr.2020.8.3.229

Hussain, M., Naeem, M.N., Asghar, S. and Tounsi, A. (2020c), "Theoretical impact of Kelvin's theory for vibration of double walled carbon nanotubes", *Adv. Nano Res.*, **8**(4), 307-322. https://doi.org/10.12989/anr.2020.8.4.307

Ibrahim, S.R. (1977), "Random decrement technique for modal identification of structures", *J. Spacecr. Rockets*, **14**(11), 696-700. https://doi.org/10.2514/3.57251.

Jacobsen, N.J., Andersen, P., and Brincker, R. (2006), "Using enhanced frequency domain decomposition as a robust technique to harmonic excitation in operational modal analysis", *Proceedings of the International Conference on Noise and Vibration Engineering* (*ISMA)*, Leuven, Belgium, September.

Juang, J.N. (1994), *Applied System Identification*, Prentice Hall, New Jersey, U.S.A.

Kalman, R.E. (1960), "A new approach to linear filtering and prediction problems", *J. Basic Eng.*, **82**(1), 35-45. https://doi.org/10.1115/1.3662552.

Kasimzade, A.A. and Tuhta, S. (2017), "Application of OMA on the bench-scale earthquake simulator using micro tremor data", *Struct. Eng. Mech.*, **61**(2), 267-274. https://doi.org/10.12989/sem.2017.61.2.267.

Kasimzade, A.A. and Tuhta, S. (2017), "OMA of model steel structure retrofitted with CFRP using earthquake simulator", *Earthq Struct.*, **12**(6), 689-697. https://doi.org/10.12989/eas.2017.12.6.689.

Lin, X., Li, M., Li, Y. and Chen, W. (2015), "Enhancement of the catalytic activity of ordered mesoporous TiO_2 by using carbon fiber support and appropriate evaluation of synergy between surface adsorption and photocatalysis by Langmuir-Hinshelwood (L–H) integration equation", *RSC Adv.*, **5**(127), 105227-105238. https://doi.org/10.1039/C5RA21083F.

Ljung, L. (1999), *System Identification: Theory for the User*, Prentice Hall, New Jersey, U.S.A.

Lus, H., De Angelis, M., Betti, R. and Longman, R.W. (2003), "Constructing second-order models of mechanical systems from identified state space realizations. Part I: Theoretical discussions", *J. Eng. Mech.*, **129**(5), 477-488. https://doi.org/10.1061/(ASCE)0733-9399(2003)129:5(477).

Ma, B., Li, H., Li, X., Mei, J. and Lv, Y. (2016), "Influence of nano-TiO_2 on physical and hydration characteristics of fly ash–cement systems", *Constr. Build. Mater.*, **122**, 242-253. https://doi.org/10.1016/j.conbuildmat.2016.02.087.

Marwala, T. (2010), *Finite Element Model Updating Using Computational Intelligence Techniques: Applications to Structural Dynamics*, Springer Science-Business Media, Berlin, Germany.

Pandey, H.K., Hirwani, C.K., Sharma, N., Katariya, P.V., Dewangan, H.C. and Panda, S.K. (2019), "Effect of nano glass cenosphere filler on hybrid composite eigenfrequency responses-An FEM approach and experimental verification", *Adv. Nano Res.*, **7**(6), 419-429. https://doi.org/10.12989/anr.2019.7.6.419

Peeters, B. (2000), "System identification and damage detection in civil engineering", Ph.D. Dissertation, Katholieke Universiteit Leuven, Leuven, Belgium.

Roeck, G.D. (2003), "The state-of-the-art of damage detection by vibration monitoring: The SIMCES experience", *J. Struct. Control*, **10**(2), 127-134. https://doi.org/10.1002/stc.20.

Sestieri, A. and Ibrahim, S.R. (1994), "Analysis of errors and

approximations in the use of modal coordinates", *J. Sound Vib.*, **177**(2), 145-157. https://doi.org/10.1006/jsvi.1994.1424.
Trifunac, M.D. (1972), "Comparisons between ambient and forced vibration experiments", *Earthq. Eng. Struct. Dyn.*, **1**(2), 133-150. https://doi.org/10.1002/eqe.4290010203.
Tseng, D.H., Longman, R.W. and Juang, J.N. (1994), "Identification of the structure of the damping matrix in second order mechanical systems", *Spaceflight Mech.*, 167-190.
Tuhta, S. (2018), "GFRP retrofitting effect on the dynamic characteristics of model steel structure", *Steel Compos. Struct.*, **28**(2), 223-231. https://doi.org/10.12989/scs.2018.28.2.223.
Tuhta, S. (2019), "OMA of model chimney using Bench-Scale earthquake simulator", *Earthq. Struct.*, **16**(3), 321-327. https://doi.org/10.12989/eas.2019.16.3.321.
Uzun, B. and Civalek, Ö. (2019), "Free vibration analysis Silicon nanowires surrounded by elastic matrix by nonlocal finite element method", *Adv. Nano Res.*, **7**(2), 99-108. https://doi.org/10.12989/anr.2019.7.2.099.
Wang, J., Liu, G., Fan, K., Zhao, D., Liu, B., Jiang, J., Qian, D., Yang, C. and Li, J. (2018), "N-doped carbon coated anatase TiO_2 nanoparticles as superior Na-ion battery anodes", *J. Colloid Interf. Sci.*, **517**, 134-143. https://doi.org/10.1016/j.jcis.2018.02.001.
Wang, L., Guo, F., Lin, Y., Yang, H. and Tang, S.W. (2020), "Comparison between the effects of phosphorous slag and fly ash on the CSH structure, long-term hydration heat and volume deformation of cement-based materials", *Constr. Build. Mater.*, **250**, 118807. https://doi.org/10.1016/j.conbuildmat.2020.118807.
Wang, L., Luo, R., Zhang, W., Jin, M. and Tang, S. (2020), "Effects of fineness and content of phosphorus slag on cement hydration, permeability, pore structure and fractal dimension of concrete", *Fractals*, **29**(2), 2140004. https://doi.org/10.1142/S0218348X21400041.
Wang, L., Jin, M., Wu, Y., Zhou, Y. and Tang, S. (2021), "Hydration, shrinkage, pore structure and fractal dimension of silica fume modified low heat Portland cement-based materials", *Constr. Build. Mater.*, **272**, 121952. https://doi.org/10.1016/j.conbuildmat.2020.121952.
Wang, L., He, T., Zhou, Y., Tang, S., Tan, J., Liu, Z. and Su, J. (2021), "The influence of fiber type and length on the cracking resistance, durability and pore structure of face slab concrete", *Constr. Build. Mater.*, **282**, 122706. https://doi.org/10.1016/j.conbuildmat.2021.122706.
Xiong, S., Yin, Z., Zhou, Y., Peng, X., Yan, W., Liu, Z. and Zhang, X. (2013), "The dual-frequency (20/40 kHz) ultrasound assisted photocatalysis with the active carbon fiber-loaded Fe_3±TiO_2 as photocatalyst for degradation of organic dye", *Bull. Korean Chem. Soc.*, **34**(10), 3039-3045. https://doi.org/10.5012/bkcs.2013.34.10.3039.
Zhang, P., Wang, K., Wang, J., Guo, J., Hu, S. and Ling, Y. (2020), "Mechanical properties and prediction of fracture parameters of geopolymer/alkali-activated mortar modified with PVA fiber and nano-SiO_2", *Ceram. Int.*, **46(**12), 20027-20037. https://doi.org/10.1016/j.ceramint.2020.05.074.
Zhang, P., Gao, Z., Wang, J. and Wang, K. (2021), "Numerical modeling of rebar-matrix bond behaviors of nano-SiO_2 and PVA fiber reinforced geopolymer composites", *Ceram. Int.*, **47**(8), 11727-11737. https://doi.org/10.1016/j.ceramint.2021.01.012.